

Effects of thermal and spin fluctuations on the band structure of purple bronze $\text{Li}_2\text{Mo}_{12}\text{O}_{34}$

T. Jarlborg, P. Chudzinski, and T. Giamarchi

DPMC-MaNEP, University of Geneva, 24 Quai Ernest-Ansermet, CH-1211 Geneva 4, Switzerland

(Received 9 March 2012; revised manuscript received 10 May 2012; published 5 June 2012)

The band structures of ordered and thermally disordered $\text{Li}_2\text{Mo}_{12}\text{O}_{34}$ are calculated by use of the *ab initio* density-functional-theory–linear-muffin-tin (DFT-LMTO) method. The unusual, very one-dimensional band dispersion obtained in previous band calculations is confirmed for the ordered structure, and the overall band structure agrees reasonably well with existing photoemission data. Dispersion and band structure perpendicular to the main dispersive direction are obtained. A temperature-dependent band broadening is calculated from configurations with thermal disorder of the atomic positions within the unit cell. This leads to band broadening of the two bands at the Fermi energy which can become comparable to their energy separation. The bands are particularly sensitive to in-plane movements of Mo sites far from the Li sites, where the density of states (DOS) is highest. The latter fact makes the effect of Li vacancies on the two bands relatively small. Spin-polarized band results for the ordered structure show a surprisingly large exchange enhancement on the high DOS Mo sites. Consequences for spin fluctuations associated with a cell doubling along the conducting direction are discussed.

DOI: [10.1103/PhysRevB.85.235108](https://doi.org/10.1103/PhysRevB.85.235108)

PACS number(s): 71.20.Gj, 75.10.Lp, 79.60.Ht, 71.10.Pm

I. INTRODUCTION

The lithium purple bronze, $(\text{Li}_{0.9}\text{Mo}_6\text{O}_{17})$ is an unusual material has drawn attention from the research community for nearly three decades.^{1,2} It is a compound with a rather complicated layered structure³ and it exhibits highly one-dimensional (1D) electronic properties.^{4–6} Indeed, band calculations starting with 3D electronic interactions reveal an electronic structure with 1D character,^{5,6} with large band dispersion only in one of the directions within the layers. The band structure shows that two bands are very close together near the crossing of the Fermi energy E_F .

Because of its 1D electronic properties, the purple bronze is a good playground on which to study the physics of one-dimensional interacting fermionic systems, which is described by the Tomonaga-Luttinger liquid (TLL) universality class.⁷ In fact, several experimental results^{8–12} are consistent with the observation of such one-dimensional physics.

However, some deviations from the simple TLL scaling are also present. Recent results from angular resolved photoemission spectroscopy (ARPES), done with very high resolution by Wang *et al.*,^{8,9} indicate some deviations from the TLL predictions. The exponents for ω and T dependence are different from the predictions, and yet another exponent is deduced from scanning tunneling measurements (STM).¹⁰

It is thus important to examine the possible sources of such deviations. One possible origin, as with any quasi-one-dimensional system, can come from the competition between strong correlations and transverse hopping in the direction perpendicular to the highly conducting axis. This will be the subject of another study.¹³ In the present paper we focus on the structural properties in the low energy limit, and examine using density functional theory (DFT) if additional ingredients should be incorporated in the previous descriptions^{5,6} based on a *rigid* band structure for the material. In particular we examine whether the thermal motion of the atoms in the solid can lead to a significant source of disorder that could blur the 1D description. Such effects, in three dimensions, are indeed important for the properties of certain classes of compounds with sharp structures of the density of states (DOS) near

E_F , such as in the B20 compound FeSi,¹⁴ and also for the appearance of the bands in other materials.^{15–17}

To achieve this goal we reexamine the band structure of the purple bronze. In order to ascertain the effects of the perpendicular hopping we compute carefully the dispersion in the transverse direction. In addition we examine the effects of thermal fluctuations and spin fluctuations.

The plan of the paper is as follows. In Sec. II we describe the method with the results for ordered structure. The effect of deviations from the ideal atomic structure, e.g., due to thermal fluctuations, are given in Sec. III. Section IV is dedicated to the effects of static, substitutional disorder. Results for spin fluctuations and a discussion of their effects are given in Sec. V. In Sec. VI we present models of how smearing and partial gaps can modify photoemission intensities.

II. BAND STRUCTURE

In this section we apply density functional band theory (DFT) in order to see to what extent it can explain the unusual photoemission data. In doing so it is important to note that the effects of thermal disorder and spin fluctuations may be important and have to be included in the density functional approach. The electronic structure of $\text{Li}_2\text{Mo}_{12}\text{O}_{34}$ (two formula units of stoichiometric purple bronze) has been calculated using the linear muffin-tin method (LMTO)^{18,19} in the local density approximation²⁰ (LDA), with special attention given to the effects of structural disorder. The lattice dimension and atomic positions of the structure have been taken from Onoda *et al.*³ The lattice constant b_0 in the conducting y direction is 5.52 Å and is more than two times larger along the least conducting x direction $a_0 = 12.76$ Å. Thus the structure consists of well separated slabs. In order to adapt the LMTO basis to an open structure such as purple bronze we inserted 56 empty spheres in the most open parts of the structure. This makes a total of 104 sites within the unit cell. The basis consists of s , p , and d waves for Mo, and s and p states for Li, O, and empty spheres, with one ℓ higher for the three-center terms. Corrections for the overlapping

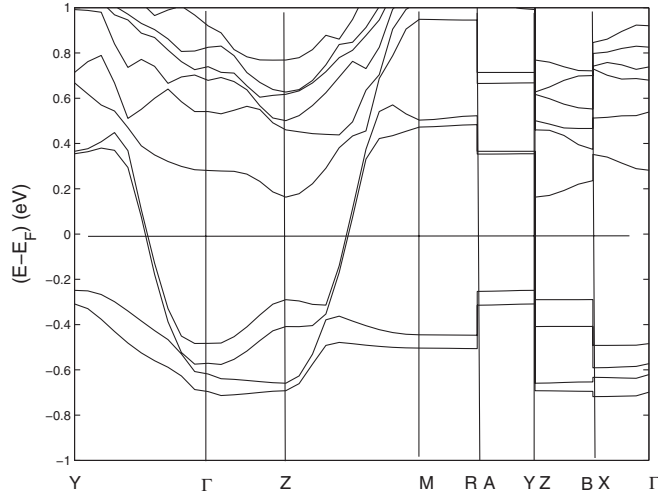


FIG. 1. Band structure of purple bronze $\text{Li}_2\text{Mo}_{12}\text{O}_{34}$ computed within DFT-LDA approximation for the rigid structure with parameters taken from Ref. 3. Bands are shown along symmetry lines in a 1 eV window around the Fermi energy E_F .

atomic spheres are included. All atomic sites are assumed to be fully occupied (except for the case with a vacant Li atom, see Sec. IV), and they are all considered as inequivalent in the calculations. Self-consistency is made using 125 k points, with more points for selected paths for the band plots.

The band structure for the undistorted structure is shown in Figs. 1–3. The total DOS at E_F , $N(E_F)$, is not very large, 2.1 states per cell and eV. The states at E_F are mainly of Mo- d character coming from sites far from the region containing Li, where locally $N(E_F)$ amounts to about 0.2 st/eV/Mo. This is less than 1/3 of $N(E_F)$ in bcc Mo.

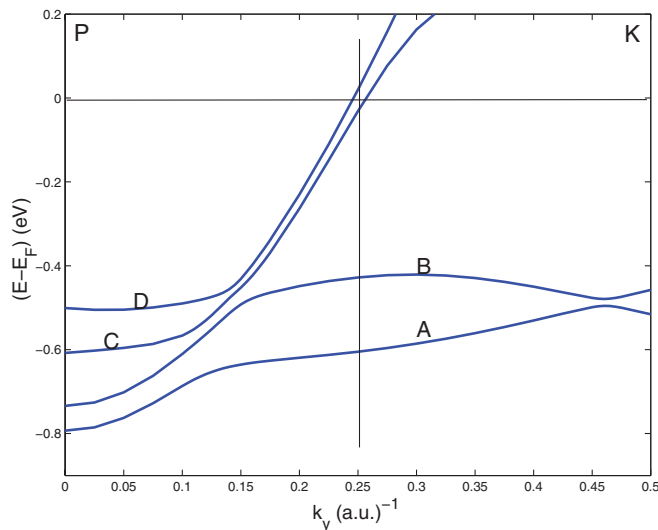


FIG. 2. (Color online) Band dispersion along P - K (parallel to Γ - Y halfway inside the zone) showing that Fermi momentum k_F is very close to half of the P - K distance (at the vertical line). The two bands crossing E_F are very close for momenta just below k_F (for details see Fig. 3) but they are separated by ~ 100 meV for $|k| \leq \frac{1}{2}|k_F|$. Notation as in Ref. 9; C and D correspond to bands 139 and 140, respectively.

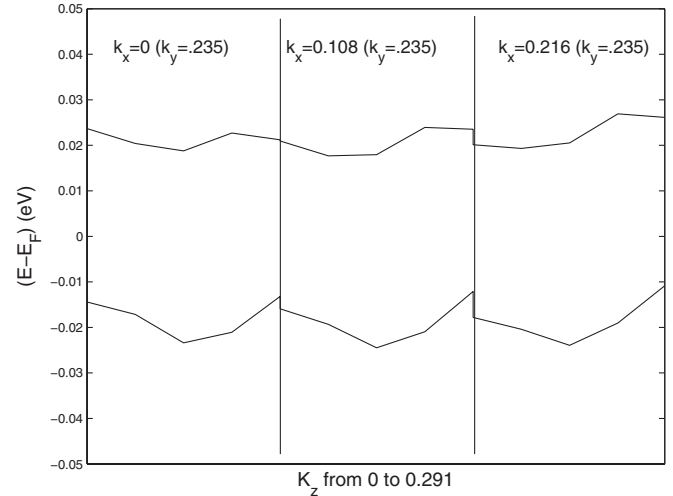


FIG. 3. Band dispersion of the two bands crossing E_F shown along the second conducting z direction. Because of lattice symmetry only a half of a dispersion curve (k values in units of $2\pi/b_0$) is shown. Three different cuts of relevant portions of the Brillouin zone are given.

Two bands, numbers 139 and 140 (counted from the lowest of the valence bands), are the only ones crossing E_F . It was already pointed out in Ref. 5 that these two bands originate from zig-zag chains (oriented along the y axis) which are grouped in pairs (along the z axis). This is the way each structural slab is built. The two bands have similar DOSs at E_F to within 10% accuracy. The Fermi velocity v_F^y along the conducting y direction is normal as for a good metal, about 5×10^5 m/s, but the ratio between the Fermi velocity in the y and z directions, about 50, is compatible with the reported anisotropic 1D-like resistivity.⁴ The velocity along \bar{x} is even smaller.²¹ The bands and the DOSs agree reasonably with the bands calculated by Whangbo and Canadell⁵ and Popović and Satpathy⁶ using different DFT methods. In Figs. 2 and 3 we show the details of the bands near E_F , where the band separation and the electronic interactions (or t integrals in a tight-binding language) can be extracted. The band dispersion along the conducting Γ - Y (or P - K) direction agrees well with the measured results obtained by ARPES⁹ showing a flattening of the two dispersive bands at about 0.4–0.5 eV below E_F . Other bands are found about 0.25 eV below E_F . The calculated structures A, B, C, and D are identified on the bands in the P - K direction in Fig. 2 at 0.6 (0.6), 0.4 (0.3), 0.6 (0.5), and 0.5 (0.4) eV below E_F , respectively, where the values within parentheses are taken from the photoemission data of Ref. 9. Thus, there is an upward shift of the order 0.1 eV in photoemission compared to the calculated bands. Such trends are typical, for instance, in ARPES on the cuprates, and can to some extent be attributed to electron-hole interaction in the excitation process.²² The overall agreement between different band results and photoemission is reassuring for this complicated structure, while we now should focus on finer details of the bands near E_F .

The 1D character of the band structure is revealed from the comparison between Figs. 1 and 3. While the band width for the bands crossing E_F is of the order 2 eV in the y direction, it is not larger than 0.02 eV along z and x . The separation between

the two bands is slightly larger, about 0.03 eV. These low values and the shape of the z and x dispersions are of importance for a Luttinger description of bands close to E_F .¹³ It should be noted that the band dispersion along the z direction is very small, and that the two bands have similar but not identical shapes, see Fig. 3. The dispersion perpendicular to the y axis is quite unusual with a minimum in the middle of the Brillouin zone instead of at $q_c = 0$. This suggests that there exist not only one but several equally important, competing hybridization paths between different chains. A brief analysis of the structure²¹ indicates that several paths are possible. First, for the closest pair of zig-zag chains there is a direct hopping between Mo(1) and Mo(4) sites, and an indirect one going through Mo(2) and Mo(5) atoms. Second, the hopping between these pairs (of chains) always has to go through Mo(2) atoms, while the next nearest neighbor hopping goes through M(2) and M(5) atoms.

The direct interchain hopping [between Mo(1) and Mo(4) sites] is weakened because it goes through a rather weak δ bond, while hoppings through M(2) and M(5) sites are enhanced because their octahedra are more distorted. The cuts along different k_b are nearly identical, which shows that this competition does not depend on the momentum of the propagating wave packet. The amplitude of the interchain hopping, computed from the band structure, shows that the one dimensionality of the compound is certain for energies above ~ 20 meV. Below this energy the question is open, because the transverse hopping can be affected by strong correlations.¹³

Another check was also made by calculating the bands for the structural a , b , and c parameters corresponding to low T . It has been reported that the thermal expansion is quite unusual, where almost no expansions are found along b and c between 0 K up to room temperature.^{23,24} A calculation for the ordered structure with all structural a parameters downscaled by 0.3%, to correspond to the structure at 0 K, was made. The effects on the bands are very small and not important for the properties discussed in this work. The average band separation decreases, but the change is not significant compared to the original band separation.

III. THERMAL DISORDER AND ZERO-POINT MOTION

The previous results were obtained by assuming an ideal periodic structure. Band structure calculations rarely take into account thermal distortions of the lattice positions. However, structural disorder due to thermal vibrations is important at high T , and properties for materials with particular fine structures in the DOS near E_F may even be affected at low T .^{14,25} Here for purple bronze, effects of thermal fluctuations might be pertinent to the degree of dimensionality and the band overlap between the two bands at E_F .

Phonons are excited thermally following the Bose-Einstein occupation of the phonon density of states $F(\omega)$. The averaged atomic displacement amplitude σ can be calculated as function of T .^{26,27} The result is approximately that $\sigma_Z^2 \rightarrow 3\hbar\omega_D/2K$ at low T due to zero-point motion (ZPM) and $\sigma_T^2 \rightarrow 3k_B T/K$ at high T (thermal excitations), where ω_D is a weighted average of $F(\omega)$. The force constant $K = M_A\omega^2$, where M_A is an atomic mass (here the mass of Mo is used because of its dominant role in the DOS), can be calculated as $K = d^2E/du^2$ (E is the total energy), or it can be taken from experiment.

We use the measurements of the phonon DOS of the related blue bronze $K_{0.3}MoO_3$ ²⁸ to estimate K and the average displacements of Mo atoms, as will be explained later.

The individual displacements u follow a Gaussian distribution function:

$$g(u) = \left(\frac{1}{2\pi\sigma^2}\right)^{3/2} \exp\left(-\frac{u^2}{\sigma^2}\right), \quad (1)$$

where σ , the standard deviation, will be a parameter in the different sets of calculations. In order to estimate the effect of such atomic displacements on the band structure, each atomic site in the unit cell is assigned a random displacement along x , y , and z following the Gaussian distribution function. Band calculations are made for a total of nine different disordered configurations. The effects will be a shift of the band position, to which both ZPM and thermal fluctuations contribute, and a broadening of the bands. Our calculation, in which we will displace atoms from their natural positions, will also give information on the nature of the band and its sensitivity to a certain type of atomic disorder.

For these investigations we have performed two types of simulations of thermal effects: first including all atoms (treated on an equal footing) and second only for atoms around the zig-zag chain where the DOS at E_F is high. In the latter case, the distortion σ_W is averaged over those sites only, see later. These calculations confirm, as expected from the static band structure, that mostly atoms around the zig-zag chains contribute to the observed effects. No general correlation between the displacements of nearest neighbors is taken into account, but extreme values of u are limited in order to avoid that two atomic spheres make a ‘‘head-on’’ collision, which of course would not occur in the real material. Further refinements of the disorder could involve different disorders for different atomic masses, and anisotropic disorder. Purple bronze is a layered material, 1D-like, and it is probable that vibrational amplitudes are different perpendicular to the planes compared to within the layers. However, such information is missing and here we assume equal isotropic disorder for all atom types. The present calculation already gives an estimate of the typical effects of such atomic displacements.

The parameter σ depends on T and the properties of the material. From the experimental data in blue bronze²⁸ we estimate the T dependence of σ for purple bronze. From this we find that σ_Z/b_0 is of the order 0.7% for Mo, and thermal vibrations become larger than σ_Z from about 120 K. For oxygen sites, σ_Z/b_0 is of the order 1%. However, as will be discussed later, the band structure is more sensitive to disorder on the Mo sites.

Two measures of the band disorder are shown in Figs. 4 and 5, both as a function of the weighted displacements σ_W , calculated as the average of distortions for the 22 sites (far from Li) with the highest $N(E_F)$. The broadening for each of the two bands is calculated from the changes in band energies $\epsilon(k)$ at 25 k points, which are found within ~ 20 meV from E_F in the undistorted case. The difference between average energy shifts of the two bands are shown in Fig. 4 as a function of σ_W . This can be thought of as a good measure of the thermally induced effects. There are more often positive energy differences, indicating that on average the two bands tend to separate because of the atoms’ random

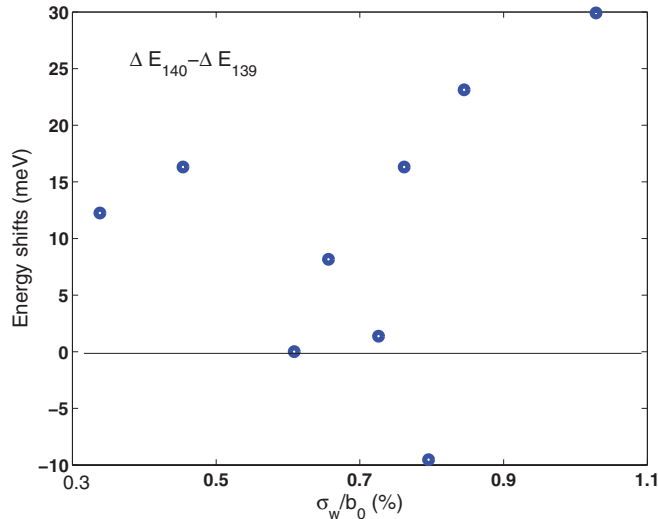


FIG. 4. (Color online) The difference of average shifts of the two bands between ordered and disordered structures as function of the site weighted disorder parameter σ_w . The zero-point motion corresponds approximately to σ_w/b_0 lower than 0.7%. There is only one point with a negative shift (near $\sigma_w/b_0 = 0.8$) which means that the two bands move closer for that particular disorder. When there is no significant average shift (e.g., for $\sigma_w/b_0 \approx 0.7$) the band broadening is only due to the internal wiggling of the bands, see Fig. 5.

displacements. The net effect is rather weak, we predict only 10 meV difference between room and helium temperature, but it could be observable. Moreover, the thermal expansion of the crystal in the b direction is anomalously weak, so it should not affect the above-mentioned result. This outcome is quite unusual, but the origin of it becomes clear when one

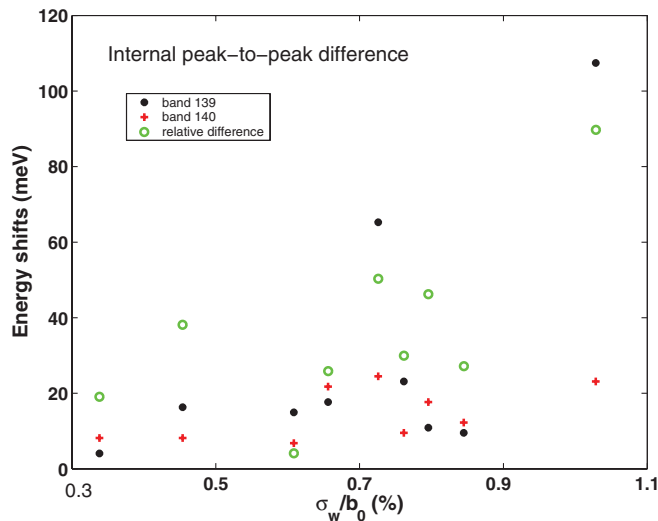


FIG. 5. (Color online) Three measures of band wiggling due to thermal distortions. Internal peak-to-peak energy differences between the bands of undistorted and distorted lattices are shown for each band (black * band 139, red + band 140). The green circles show the maximal relative difference *between* the two bands [see Eq. (3)]. The site weighted disorder parameter σ_w is defined in the text.

analyzes the structure of a crystal. It has been suggested⁵ that the t_{\perp} hopping along the c axis is particularly weak in purple bronze because of certain cancellations in hopping integrals (the δ bonds mentioned in Sec. II), when the ions reside in high symmetry points. Our finding puts that statement on firm ground: we clearly notice that when ions are slightly shifted, the perpendicular hopping can benefit noticeably.

We can gain even more information when studying the internal behavior of the two bands separately. Measures of the “wiggling” of each band because of disorder are displayed in Fig. 5. Peak-to-peak differences are given by

$$\Delta E_{\max}^j = |\max[\Delta\epsilon^j(k_n)] - \min[\Delta\epsilon^j(k_n)]|, \quad (2)$$

$j = 139$ or 140 , where $\Delta\epsilon^j(k_n)$ is the deviation in energy (with respect to undistorted band) at a certain point k_n for band j . The search for extremes goes through the set of k points k_n ($n = [1, 25]$). These differences of extremes are shown for the two bands. For the largest disorder, band 139 has changed some 100 meV at one k point relative to the change of the same band at some other k point; however, this quite large value has to be taken with caution. In general the bands’ wiggling is of the same order as the average difference between the two bands (shown on Fig. 4). We suspect that the origin of wiggling is the same as the origin of increased band separation, namely, the activation of certain overlap integrals. However, the fact that the wiggling is equally as strong as the band splitting implies that, at least within naive tight-binding interpretation, either the interladder hopping is equally strong or that the next nearest neighbor hopping is of the same order as the standard t_{\perp} . This second implication goes along the same lines as the ones discussed in the context of Fig. 3.

The lower band appears to be more sensitive than the upper band in this respect. The third quantity shown in Fig. 5 is the maximum difference

$$\Delta\epsilon = \max|\Delta\epsilon^{139}(k_n) - \Delta\epsilon^{140}(k_n)|. \quad (3)$$

It is defined as the relative band deviation at a certain point k_n . A particular case is if the two bands would change in the same way because of thermal disorder (e.g., shift homogeneously), then this last value would be equal to the absolute value of what is shown in Fig. 4. This is not the case, which means that the two bands will change quite independently of each other. In other words, most of the k points are concerned with the energy changes, and the wiggling of the two bands is different. The interpretation of this subtle difference, not visible within standard DFT band structure results, is quite difficult. It implies that bands 139 and 140 do not have identical site dependence. In other words one should not naively assume that they originate from two zig-zag chains which are very weakly hybridized as is commonly done in the literature. The microscopic complexity of effective interactions, at least at the lowest energy scales of order ~ 10 meV, needs to be rich.

In our calculation we have considered displacements of all sites, but the bands at E_F are mostly sensitive to disorder of Mo sites with a high DOS. This is reflected by calculations in which *only* the four Mo with the highest DOS are displaced 0.7% of b_0 in a few selected directions. When these sites are displaced perpendicular to the diagonal (\vec{x}, \vec{z}) direction the average band shift (equivalent to the shifts displayed in Fig. 4 for general disorder) is about 10 meV, while if the displacement is in the

directions parallel to the diagonal the shift is about 50 meV. The effect of movements in the \bar{y} directions is typically one order of magnitude smaller. This indicates that the phonon mode with displacements of Mo(4) and Mo(1) atoms (the sites from the same chain) towards each other is strongly coupled to the electronic liquid.

These values of energy changes can be compared with the distance between the bands near E_F in the undistorted case, shown above in Fig. 3 for the relevant paths in k space. The undistorted bands are separated by 30–40 meV, and the two bands are confined within 10–15 meV along k_x and k_z . The additional wiggling for distorted cases is of the same order, 20–40 meV, as seen in Fig. 5. However, this effect coexists with a (smaller) increase of the band separation. The band separation will generally increase when thermal fluctuations are at play. This is an indication of increased electronic delocalization within the layers towards a more 3D band structure, but this also indicates that any disorder will strongly affect carrier propagation along the c axis. As the temperature increases, the thermal fluctuation effects will increase which means that if this picture is valid, the experimentally observed band broadening should noticeably increase with temperature. This becomes specially important when thermal activation of phonons becomes dominant at about 120 K. In addition, the relatively rapid dispersion along k_y makes the band overlap important in k space. For instance, a band separation of 25 meV corresponds to a shift of k_y of only 0.01 of the Γ - Y distance.

IV. STATIC DISORDER

In addition to the thermal effects, on which we concentrated in the previous section, disorder can come from a variety of other sources. In particular, imperfections of the crystal (from nonstoichiometry, vacancies, site exchange, etc.) should also contribute to the effect. One can also worry about the fact that one out of ten Li atoms are missing in the real material. The unit cell considered here contains two Li, and the influence on the electronic bands from the replacement of one of these with an empty sphere (without taking structural distortion into account) is moderately large. The Fermi level goes down because one electron is removed, but if one neglects the chemical potential shift it leads to an increase of the average band separation between bands 139 and 140 by about 40 meV. This is comparable to the largest calculated effects of thermal disorder, see Fig. 4. However, a more realistic estimate is obtained in virtual crystal calculations where one of the Li is replaced by a virtual atom with nuclear and electron charges of 2.8 (instead of 3.0 for the other Li). This setup has the correct electron count corresponding to 90% occupation of Li. Now the average shifts of the two bands is much smaller, and the wiggling of the bands are not even comparable (\sim less than half) to what is found from ZPM. Therefore it can be expected that effects from thermal disorder will overcome those from structural disorder in high quality samples.

The smallness of this effect has important implications if one looks from the 1D Luttinger liquid perspective. The random Li vacancies are placed relatively far from zig-zag chains where 1D liquid resides. This implies that the interaction will have Coulomb character, the small momentum exchange events shall dominate. Thus substitutional disorder

will have primarily forward scattering character with an amplitude ≈ 15 meV as determined above. This situation can be modeled as a Luttinger liquid with forward disorder. In this case the spectral function can be given.¹³ This implies that substitutional disorder cannot be invoked to explain phenomena taking place at energy scales larger than 15 meV. For these larger energies the standard Luttinger liquid behavior is expected.

V. SPIN FLUCTUATIONS

In Figs. 1 and 2 it is seen that the two free-electron-like bands cross E_F very close to half of the Γ - Y or P - K distance along the conducting \bar{y} direction of the structure. A doubling of the real space periodicity in this direction would open a gap in the DOS near E_F and lead to a gain in total energy,^{29–32} suggesting that this material might have intrinsic spin-density wave type instabilities. In strongly correlated materials, solving these questions is of course complicated, specially in a low-dimensional material, since the proper spin exchanges and quantum fluctuations have to be taken into account. Some of these issues can be addressed at the level of the microscopic model derived in Ref. 13. Here we look at the possibility of such a spin instability, at the band structure level and low temperatures, where the two- and three-dimensional aspects of the system can *a priori* play a more important role, and thus the effect of interactions can be reduced.⁷

A complete verification of how a cell doubling with phonons or magnetic waves affects the band near E_F would require more complex band calculations, and will be a demanding undertaking. Instead we propose at this stage to extract information from calculations for the 104-site cell, and to apply a free electron model of the band dispersion in the y direction to see if magnetic fluctuations might be of interest for a band gap. We noted that displacements of some Mo with the highest local $N(E_F)$ contribute much to the band distortion. But the sizes of the potential shifts at these sites are limited by rather conservative force constants. Therefore, even if a selected phonon can contribute to a gap near E_F , it might be more effective to open gaps through spin waves since the potential shifts in this case can diverge near a magnetic instability. In order to estimate the strength of the exchange enhancement on Mo we extend our calculations for the ordered structure to be spin polarized with an antiferromagnetic spin arrangement of the moments on the Mo with the highest $N(E_F)$. This is made by application of positive or negative magnetic fields within the atomic spheres of two groups of four Mo in the cell with the highest DOS.

The propensity for fluctuations of antiferromagnetic moments within the cell is surprisingly large according to the calculations. The local exchange enhancement on Mo, corresponding to the Stoner factor for ferromagnetism (i.e., the ratio between exchange splitting and applied magnetic field), is close to 4.5 in calculations at low field and temperature. The total energy $E(m)$ is fitted to a harmonic expansion of the moment amplitude m , $E_m = K_m m^2$, where K_m is the “force constant.” In analogy with phonon displacement amplitudes one can estimate $m^2 = k_B T / K_m$ as a measure of the amplitude of moment fluctuations.³³ While phonon distortions u always increase with T , in a Fermi liquid framework one expects that

magnetic moments m will be quenched at a certain T .²⁹ This is because of a self-supporting process where m is a function of the exchange splitting ξ . The latter depends on m and the local spin density, and the mixing of states above and below E_F given by the Fermi-Dirac function will reduce m at high T , so m and ξ can drop quite suddenly. Calculations at an electronic temperature of 200 K make $K_m \approx 2\text{eV}/\mu_B^2$. From this one can estimate that m will be of the order $0.1 \mu_B$ per Mo at room temperature, which corresponds to $\xi \approx 0.2 \text{ eV}$. Another complication is that the thermal disorders of the lattice are mixing states across E_F , too, and this is another diminishing factor for spin polarization. Nevertheless, it suggests that spin fluctuations can play a role at low or intermediate temperatures. It is interesting to note that the value of ξ is of the same order of magnitude as the superexchange parameter calculated from strong correlations.^{13,34} If one compares this value with the previously determined strength of disorder and effects of thermal fluctuations, one would realize that spin fluctuations play a much more prominent role in the low energy physics. Such fluctuations can potentially lead to pseudogap features in the band dispersion, thus understanding better their properties is an interesting challenge, clearly going way beyond the scope of this paper. On the experimental side, there was only one report of such large gap ($\Delta > 10 \text{ meV}$) in the low energy spectrum¹¹ and in the light of more recent experiments¹² done with the same method this finding is highly controversial. An extremely small gap has been observed in transport experiments,³⁵ and probably in STM;¹⁰ however, the spin sector probed by static susceptibility^{4,36} and muon spectroscopy³⁷ certainly is not gapped. Further theoretical studies are necessary to understand this situation, where high magnetic propensity does not lead to a gap for spin excitations.

VI. COMPARISON WITH ARPES

We show in this section some of the consequences of the band structure calculated above for the ARPES data. Note that the above calculation does not take into account the effects of strong correlations. Thus a deviation from the picture presented below should be a direct measure and consequence of such effects. This will of course depend on the range of temperature and/or energy.

In order to simulate ARPES intensities for the free electron bands near E_F we ignore matrix elements and energy relaxations due to electron-hole interactions. We consider one-particle excitations directly from the band occupied according to the Fermi-Dirac distribution, and with pyramidal broadening functions for energy (experimental and intrinsic broadening due to disorder) and momentum k . The experimental broadenings have the same FWHM values as in the work of Wang *et al.*, and we chose to show cuts in momentum of the same step size as in their work.⁹ The free electron band is fitted to the LMTO results so that E_F is 0.6 eV at k_F . The splitting into two bands of $\sim 30 \text{ meV}$ is assumed constant everywhere, which is approximately true for the real bands near E_F . A linear background is added to the intensities in order to make a more realistic display of photoemission with secondary excitations. Five cuts in momentum below k_F , in equal steps as in Ref. 9, descend to about -0.2 eV . The five cuts

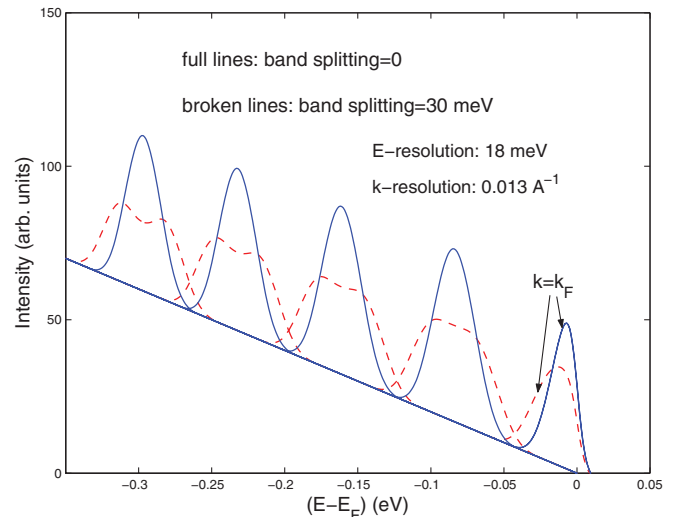


FIG. 6. (Color online) Free electron intensities for 5 k values going from k_F in steps of 3.6% of Γ - Y added to an arbitrarily chosen background. The energy and momentum resolutions ΔE and Δk are similar to the experimental values in Ref. 9. It is seen that a band splitting of more than $\sim 30 \text{ meV}$ should be seen in photoemission.

appear almost equally spaced in energy, since the dispersion is almost linear within the narrow energy interval.

First, as shown in Fig. 6, the band splitting of about 30 meV should be visible in the ARPES data if only the experimental broadening functions are at work. Second, the broken lines in Fig. 7 show wider distributions, because of additional broadening coming from the thermal disorder of the lattice. These distributions are not as wide as in Ref. 9. This strongly suggests that other physical effects (effects of interactions, static disorder due to nonstoichiometry, spin fluctuations) are at play.

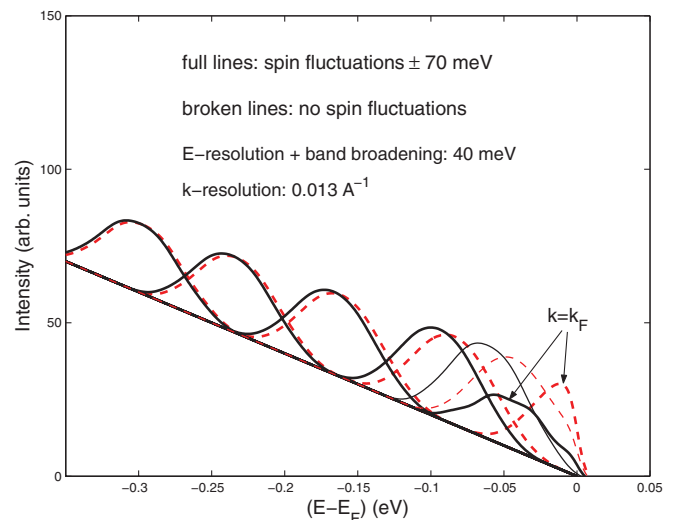


FIG. 7. (Color online) Calculated intensities for a band splitting of 30 meV as in Fig. 6, but where a band broadening of $\sim 25 \text{ meV}$ has been included (broken lines). One intermediate cut with k at 1.8% from k_F is added in this figure. The band broadening makes the band splitting undetected. Full lines: Including spin fluctuations as described in the text. Note the energy lowering close to E_F .

As an extreme case we can consider a cell doubling (e.g., due to spin ordering) which would create a gap near $k_y = k_F$. The full lines in Fig. 7 show what would happen to the spectra if ξ in the free electron model goes up to about 70 meV. In this case it is seen that the band retracts from E_F , since the peaks for k closest to k_F are lower in energy than the broken lines. Far below E_F there is not much difference between full and broken lines. In the end the presence of a gap leads to a more nonuniform energy distribution of the five k cuts of the intensity. Comparison of the experimental features with the one obtained by such a band structure analysis could thus be useful to investigate the low energy properties of purple bronze, and in particular the existence of a gap or pseudogap in the dispersion relation. The analysis in Ref. 9 revealed a $T^{0.6}$ scaling of the intensity near E_F over a wide T interval. It is important to ascertain whether this behavior at low energy comes from one-dimensional fluctuations or some pseudogap regime.

VII. CONCLUSION

In this paper we have reexamined the band structure of purple bronze in the ordered lattice and found that the main features of the bands agree well with previous calculations and ARPES results. In particular, only two bands cross the Fermi level. In our study we focus on these two bands. The perpendicular interactions along z and x (“perpendicular hoppings”) are weak and appear to lay out the conditions of TLL-like behavior of the bands near E_F , for energy down to at least 20 meV.

We have investigated whether additional effects giving small energy distortions at these energy scales could cause an overlap between these two bands at low T . The energy separation between the two essentially one-dimensional bands increases below E_F , as can be seen in Fig. 1 along the Γ - Y direction. For instance, the two considered bands are separated ~ 0.1 eV at 0.4 eV below E_F , similar to what is seen in ARPES at this energy.⁹ When bands are closer to E_F then they are also closer together; however, as shown in Sec. VI within a single-particle picture (LDA-DFT) they should be distinguishable at low T provided that intrinsic disorder is not too large and if the matrix elements for transitions from both bands are comparable.³⁸ As T increases beyond ~ 120 K or more, the band broadening increases because of additional thermal disorder so that the two bands seem to merge. We find that the thermal effects can potentially play a role in the band separations; however, one has to keep in mind the temperature dependence of the effect: the bands become less

and less distinguishable as the temperature increases. There is obviously a complicated cooperation between increase in splitting and wiggling, but in any case the following effect can be used to verify experimentally this picture: as the temperature increases, the ARPES lines should become noticeably thicker.

Additional calculations for Li deficient purple bronze show no important modifications of the bands crossing E_F , at least as long as it is not associated with static disorder. Likewise the band structure for a unit cell with modified x/y and x/z ratios, appropriate for the structure at room temperature, is not very different from what is shown in Fig. 1.

Recent photoemission results of Wang *et al.*,⁹ made at low T , only detect one band at E_F . The interpretation of these results is still an exciting issue given the fact that electron-electron interactions can also suppress tunneling and reinforce the one dimensionality of the material.¹³ What we showed in this paper is that at a one-body level, the effect of distortion of the electronic structure also goes in the direction of a smearing of the difference between the two bands and thickening observed in ARPES spectra. Disentangling the two effects is thus important and can potentially be done by comparing the predicted band separations, at the level of band structure, with the actual ARPES data.

We have also explored the possibility of antiferromagnetic spin fluctuations. Here, our investigations are not complete, but our first results show surprisingly large antiferromagnetic exchange enhancements on Mo within the basic unit cell. This and other facts motivate further studies of fluctuations within larger cells in order to see if they can lead to gap or pseudogap features near E_F .

It is interesting to note that the existence of thermal fluctuations and imperfections of the atomic structure, makes—at the band structure level—the system more three dimensional. This effect will be in competition with the renormalization of the interchain hopping coming from the electron-electron correlations. The competition between these two effects leads to an intermediate and low temperature physics which is still mysterious in this compound.

ACKNOWLEDGMENTS

We are grateful to J. W. Allen and E. Canadell for sharing their knowledge about purple bronze. We also acknowledge exchange of useful information from S. Satpathy, T. Saha-Dasgupta, M. W. Haverkort, and J. D. Denlinger. This work was supported by the Swiss NSF under MaNEP and Division II.

¹W. H. McCarroll and M. Greenblatt, *J. Solid State Chem.* **54**, 282 (1984).

²C. Schlenker, H. Schwenk, C. Escribe-Filippini, and J. Marcus, *Physica B* **135**, 511 (1985).

³M. Onoda, K. Toriumi, Y. Matsuda, and M. Sato, *J. Solid State Chem.* **66**, 163 (1987).

⁴M. Greenblatt, W. H. McCarroll, R. Neifeld, M. Croft, and J. V. Waszczak, *Solid State Commun.* **51**, 671 (1984).

⁵M.-H. Whangbo and E. Canadell, *J. Am. Chem. Soc.* **110**, 358 (1988).

⁶Z. S. Popović and S. Satpathy, *Phys. Rev. B* **74**, 045117 (2006).

⁷T. Giamarchi, *Quantum Physics in One Dimension* (Oxford University, Oxford, England, 2004).

⁸F. Wang, J. V. Alvarez, S.-K. Mo, J. W. Allen, G. H. Gweon, J. He, R. Jin, D. Mandrus, and H. Höchst, *Phys. Rev. Lett.* **96**, 196403 (2006).

- ⁹F. Wang, J. V. Alvarez, J. W. Allen, S.-K. Mo, J. He, R. Jin, D. Mandrus, and H. Höchst, *Phys. Rev. Lett.* **103**, 136401 (2009).
- ¹⁰J. Hager, R. Matzdorf, J. He, R. Jin, D. Mandrus, M. A. Cazalilla, and E. W. Plummer, *Phys. Rev. Lett.* **95**, 186402 (2005).
- ¹¹J. Xue, L. C. Duda, K. E. Smith, A. V. Fedorov, P. D. Johnson, S. L. Hulbert, W. McCarroll, and M. Greenblatt, *Phys. Rev. Lett.* **83**, 1235 (1999).
- ¹²G.H. Gweon, J.D. Denlinger, J.W. Allen, C.G. Olson, H. Hoehst, J. Marcus, and C. Schlenker, *Phys. Rev. Lett.* **85**, 3985 (2000).
- ¹³P. Chudzinski, T. Jarlborg, and T. Giamarchi, arXiv:1205.0239.
- ¹⁴T. Jarlborg, *Phys. Rev. B* **59**, 15002 (1999).
- ¹⁵R. H. McKenzie and J. W. Wilkins, *Phys. Rev. Lett.* **69**, 1085 (1992).
- ¹⁶F. Giustino, S. G. Louie, and M. L. Cohen, *Phys. Rev. Lett.* **105**, 265501 (2010).
- ¹⁷E. Cannuccia and A. Marini, *Phys. Rev. Lett.* **107**, 255501 (2011).
- ¹⁸O. K. Andersen, *Phys. Rev. B* **12**, 3060 (1975).
- ¹⁹T. Jarlborg and G. Arbman, *J. Phys. F* **7**, 1635 (1977); B. Barbiellini, S. B. Dugdale, and T. Jarlborg, *Comput. Mater. Sci.* **28**, 287 (2003).
- ²⁰W. Kohn and L. J. Sham, *Phys. Rev.* **140**, A1133 (1965).
- ²¹We adopt the same conventions as in Refs. 3 and 6 for the structure, site notation, and k space, so that \vec{x} and \vec{z} are parallel and \vec{y} perpendicular to the planes.
- ²²T. Jarlborg, B. Barbiellini, H. Lin, R. S. Markiewicz, and A. Bansil, *Phys. Rev. B* **84**, 045109 (2011).
- ²³C. A. M. dos Santos, B. D. White, Y.-K. Yu, J. J. Neumeier, and J. A. Souza, *Phys. Rev. Lett.* **98**, 266405 (2007).
- ²⁴M. S. daLuz, J. J. Neumeier, C. A. M. dos Santos, B. D. White, H. J. I. Filho, J. B. Leao, and Q. Huang, *Phys. Rev. B* **84**, 014108 (2011).
- ²⁵P. Pedrazzini, H. Wilhelm, D. Jaccard, T. Jarlborg, M. Schmidt, M. Hanfland, L. Akselrud, H.Q. Yuan, U. Schwarz, Y. Grin, and F. Steglich, *Phys. Rev. Lett.* **98**, 047204 (2007).
- ²⁶G. Grimvall, *Thermophysical Properties of Materials* (North-Holland, Amsterdam, 1986).
- ²⁷J. M. Ziman, *Principles of the Theory of Solids* (Cambridge University, New York, 1971).
- ²⁸H. Requardt, R. Currat, P. Monceau, J. E. Lorenzo, A. J. Dianoux, J. C. Lasjaunias, and J. Marcus, *J. Phys. Condens. Matter* **9**, 8639 (1997).
- ²⁹T. Jarlborg, *Physica C* **454**, 5 (2006).
- ³⁰R. E. Peierls, *Quantum Theory of Solids* (Oxford University, Oxford, England, 1955).
- ³¹G. Beni and P. Pincus, *J. Chem. Phys.* **57**, 3531 (1972).
- ³²E. Pytte, *Phys. Rev. B* **10**, 4637 (1974).
- ³³T. Jarlborg, *Phys. Rev. B* **79**, 094530 (2009).
- ³⁴S. Nishimoto, M. Takahashi, and Y. Ohta, *J. Phys. Soc. Jpn.* **69**, 1594 (2000).
- ³⁵X. Xu, A. F. Bangura, J. G. Analytis, J. D. Fletcher, M. M. J. French, N. Shannon, N. E. Hussey, J. He, S. Zhang, D. Mandrus, and R. Jin, *Phys. Rev. Lett.* **102**, 206602 (2009).
- ³⁶J. Choi, J. L. Musfeldt, J. He, R. Jin, J. R. Thompson, D. Mandrus, X. N. Lin, V. A. Bondarenko, and J. W. Brill, *Phys. Rev. B* **69**, 085120 (2004).
- ³⁷J. Chakhalian Z. Salman, J. Brewer, A. Froese, J. He, D. Mandrus, and R. Jin, *Physica B* **359**, 1333 (2005).
- ³⁸In Ref. 9 the intensity of the upper band is much lower than that of the lower one.